

See discussions, stats, and author profiles for this publication at: <https://www.researchgate.net/publication/234956950>

Interaction of cyclobutane with the Ru(001) surface: Low-temperature molecular adsorption and dissociative chemisorption at elevated surface temperature

ARTICLE *in* THE JOURNAL OF CHEMICAL PHYSICS · JANUARY 1999

Impact Factor: 2.95 · DOI: 10.1063/1.477811

CITATIONS

7

READS

12

6 AUTHORS, INCLUDING:



Chan-Hwa Chung

Sungkyunkwan University

101 PUBLICATIONS 1,535 CITATIONS

SEE PROFILE

Interaction of cyclobutane with the Ru(001) surface: Low-temperature molecular adsorption and dissociative chemisorption at elevated surface temperature

Christopher J. Hagedorn and Michael J. Weiss

Department of Chemical Engineering, University of California, Santa Barbara, Santa Barbara, California 93106-5080

C.-H. Chung

Department of Chemical Engineering, Seoul National University, Shinlin-Dong, Kwanak-Ku, Seoul, Korea 151-742

Peter J. Mikesell and R. Daniel Little

Department of Chemistry, University of California, Santa Barbara, Santa Barbara, California 93106-9510

W. Henry Weinberg

Department of Chemical Engineering and Department of Chemistry, University of California, Santa Barbara, Santa Barbara, California 93106-9510

(Received 13 August 1998; accepted 12 October 1998)

We have studied the interaction of cyclobutane with the hexagonally close-packed Ru(001) surface. High-resolution electron energy loss spectroscopy (HREELS) has been used to identify the vibrational modes of both *c*-C₄H₈ and *c*-C₄D₈ adsorbed at 90 K as a function of cyclobutane exposure. We have observed a vibrational mode not observed in the gas phase at 2600 cm⁻¹ (2140 cm⁻¹) which is attributed to the strong interaction of the cyclobutane C–H (C–D) bonds with the ruthenium surface. Two different adsorption geometries for cyclobutane on Ru(001) have been proposed based on the dipolar activity of this softened C–H mode. We have also measured the trapping-mediated dissociative chemisorption of both *c*-C₄H₈ and *c*-C₄D₈ at surface temperatures between 190 and 1200 K. The measured activation energies with respect to the bottom of the physically adsorbed well for *c*-C₄H₈ and *c*-C₄D₈ are 10 090±180 and 10 180±190 cal/mol, respectively. The trapping-mediated chemisorption of cyclobutane is believed to occur via C–C bond cleavage, as judged by the absence of a kinetic isotope effect. The measured ratios of the preexponential factors for desorption relative to reaction of 21±2 and 47±4 for *c*-C₄H₈ and *c*-C₄D₈ respectively, are in the expected range considering the greater entropy gain associated with the transition state for desorption relative to the transition state for C–C bond cleavage. © 1999 American Institute of Physics. [S0021-9606(99)70103-0]

I. INTRODUCTION

Adsorption and reaction of hydrocarbons on transition metal surfaces are of great scientific interest, especially to the field of heterogeneous catalysis research, due to the technological importance of hydrocarbons as fuel sources and as building blocks in the production of value-added chemicals. Therefore, fundamental investigations concerned with understanding microscopic processes such as adsorption, desorption, diffusion, and reaction of hydrocarbons on these surfaces are crucial for fully understanding the phenomena which occur on a macroscopic level. In particular, there have been hundreds of studies concerned with quantifying the reaction probabilities of light hydrocarbons on transition metal surfaces. These studies have provided a great deal of fundamental information concerning the reactivity and selectivity of various hydrocarbons on a number of catalytically active transition metal surfaces. The results of Johnson and Weinberg^{1,2} involving measurements of the kinetic parameters for cleavage of both C–C and C–H bonds in propane on the Ir(111) surface are particularly relevant in this regard.

It was possible to quantify separately the activation energies and preexponential factors of the reaction rate coefficients for C–C bond cleavage, primary C–H bond cleavage, and secondary C–H bond cleavage. In a similar manner, we have measured the reaction probability of cyclobutane on the hexagonally close-packed Ru(001) surface as a function of surface temperature with the aim of obtaining the kinetic parameters that describe this reaction. One of the primary goals of this work is to determine whether the initial dissociative chemisorption of cyclobutane occurs via C–H or C–C bond cleavage.

Cyclobutane is an interesting molecule due to the Baeyer strain (bond angle strain), Pitzer strain (torsional strain), and Dunitz–Schomaker strain (1,3 CC interactions) which are present due to the molecular geometry of cyclobutane.³ The C–C–C bond angles of cyclobutane of approximately 90° deviate from the standard strain-free C–C–C bond angle by 19.5°. As a result of this strained geometry, the C–C bonds in cyclobutane are slightly weaker, and the C–H bonds are slightly stronger than those in an unstrained alkane. For cyclopropane, which has an overall strain energy very close to

that of cyclobutane,^{3,4} Jachimowski *et al.*⁵ have recently determined that the dissociative chemisorption on Ru(001) occurs via C–C bond cleavage. Therefore, a relevant question is whether or not cyclobutane follows this same reaction pathway of C–C bond cleavage on Ru(001).

In this study we have also employed HREELS with the aim of providing information regarding the geometry of physically adsorbed cyclobutane on the Ru(001) surface at 90 K. We have proposed two possible adsorption geometries for cyclobutane which are consistent with the vibrational spectra. Our goal is to combine the information obtained from these vibrational spectra with the kinetic data which describe the activation of cyclobutane at elevated surface temperature in order to develop a complete understanding of the interaction of cyclobutane with the Ru(001) surface.

II. EXPERIMENTAL METHODOLOGIES

The experiments were carried out in a stainless steel ultrahigh vacuum chamber (base pressure of 7×10^{-11} Torr) equipped with HREELS, Auger electron spectroscopy (AES), low-energy electron diffraction (LEED), x-ray photoelectron spectroscopy (XPS), a twice differentially pumped radical beam source, and a differentially pumped quadrupole mass spectrometer for temperature programmed desorption (TPD) measurements.^{6–8} The HREEL spectra were acquired using a commercial LK-2000 HREEL spectrometer (LK Technologies), the resolution of which varied between 50 and 70 cm^{-1} (full width at half maximum of the elastically scattered beam) while maintaining a counting rate of at least 5×10^4 Hz in the elastically scattered peak in the specular direction.

The Ru(001) single crystal sample was mounted on a homebuilt cryostat that can cool the sample to 90 K using liquid nitrogen. The temperature of the crystal could be varied from 90 to 1700 K by resistive heating; the sample temperature was monitored using a type-C thermocouple that was spotwelded to the back of the crystal. The surface was cleaned using standard methods of Ar^+ sputtering as well as annealing to 1550 K in a background of oxygen. The crystal was heated to 1650 K in order to remove all chemisorbed oxygen,⁹ and surface cleanliness was verified by HREELS, LEED, carbon monoxide TPD, and AES. The sample temperature was always kept below 800 K, except in the presence of adsorbed oxygen, in order to prevent the formation of graphite on the surface.

Cyclobutane and cyclobutane- d_8 were synthesized via Wurtz coupling¹⁰ reactions in which 1,4-dibromobutane and 1,4-dibromobutane- d_8 were used as starting materials. Lithium shot (2.19 g, $-4+16$ mesh) in mineral oil was added to a dry 250 ml round bottom flask, and the mineral oil was removed by washing with three 5 ml aliquots of hexanes, after which the residual hexane was purged by passing a stream of argon through the flask. Next, mercury (448 g) was added to the lithium. A condenser, Claisen adapter, and a gas trap were then added to the apparatus. Warm tap water (40°C) was circulated through the condenser and the reaction was carried out under an argon atmosphere. Lithium mercury amalgam was generated by gently heating the flask until the lithium dissolved. 1,4-dioxane (135 ml), freshly dis-

tilled from sodium, was added to the round bottom flask. The gas trap was cooled in a dry ice–acetone bath. The 1,4-dioxane was brought to reflux and a solution of 89 mmol of 1,4-dibromobutane in 19 ml of dioxane was added dropwise over 30 min. The 1,4-dioxane was allowed to reflux for six hours, while cyclobutane was collected in the gas trap. The cyclobutane product was then purified to greater than 99% purity (as verified by mass spectrometry) by performing several freeze–pump–thaw cycles on our gas-handling manifold.

For TPD and HREELS experiments involving cyclobutane adsorption at low temperature, cyclobutane was background dosed onto the clean Ru(001) sample at a surface temperature of 90 K. Cyclobutane exposures between 0.35 and 20 L [$1 \text{ Langmuir (L)} = 1 \times 10^{-6} \text{ Torr s}$] were obtained by continuously flowing cyclobutane into the ultrahigh vacuum (UHV) chamber at pressures between 1×10^{-8} and 1×10^{-7} Torr (uncorrected for ion gauge sensitivity) for times ranging between 35 and 200 s.

The initial probability of trapping-mediated dissociative chemisorption of cyclobutane on Ru(001) was measured by continuously flowing cyclobutane into the chamber at a pressure of 1×10^{-8} Torr (uncorrected for ion gauge sensitivity) for times between 100 and 400 s while holding the crystal at a constant temperature between 190 and 1200 K. These exposures were selected such that the coverage of carbon adatoms left on the surface following the dissociation of cyclobutane was between 4% and 10%. The lower limit was chosen to guarantee that activation at surface defect sites did not dominate the overall reaction probability, while the upper limit was selected in order to approximate a measurement of the initial probability of dissociative chemisorption. Immediately following each cyclobutane exposure, the sample was cooled to 90 K, the ruthenium surface was exposed to 10 L of molecular oxygen (Matheson, 99.9999%), and a TPD experiment was performed. This resulted in the desorption of reaction-limited CO which was formed by the reaction of oxygen and carbon adatoms. Using this method,^{5,11} the ratio of CO to CO_2 production was ~ 100 . The background adsorption of CO onto the surface during exposure of the oxygen was found to be negligible. The surface coverage of carbon adatoms, θ_C (number of carbon atoms per surface ruthenium atom), deposited by the dissociation of cyclobutane, was calculated by comparing the time-integrated area of the reaction-limited CO desorption in each experiment to the desorption of a saturation coverage of CO on Ru(001), $\theta_{\text{CO,sat}} = 0.67$.^{12,13}

Since the reaction probability of cyclobutane is proportional to the surface coverage of atomic carbon deposited on the surface, we can write the probability of reaction, P_r , at a given surface temperature, T_s , as

$$P_r = \frac{\theta_C N_s}{4F\tau}, \quad (1)$$

where N_s is the number of Ru(001) surface sites per unit area ($1.57 \times 10^{15} \text{ sites/cm}^2$), the factor of 4 accounts for the number of carbon atoms in a cyclobutane molecule, F is the impingement rate of cyclobutane molecules onto the surface per unit area, and τ is the exposure time.

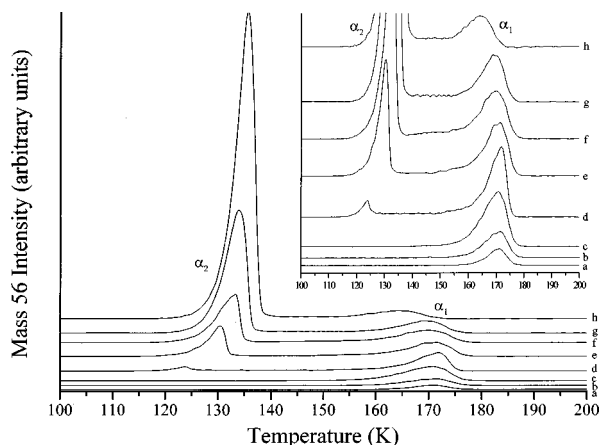


FIG. 1. TPD spectra of $m/e=56$ (C_4H_8) collected after exposure of the clean Ru(001) surface to cyclobutane exposures of [in Langmuir (L)]: (a) 0.35, (b) 0.7, (c) 1.5, (d) 2.0, (e) 3.5, (f) 5.0, (g) 10.0, and (h) 20.0. The heating rate for all spectra is 5 K/s.

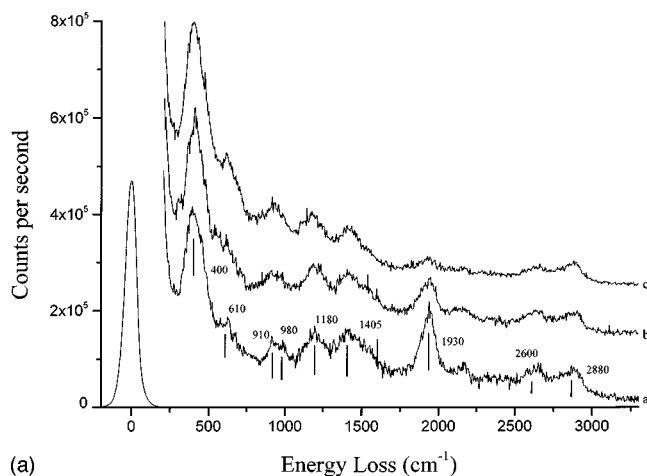
III. RESULTS AND DISCUSSION

A. Temperature programmed desorption

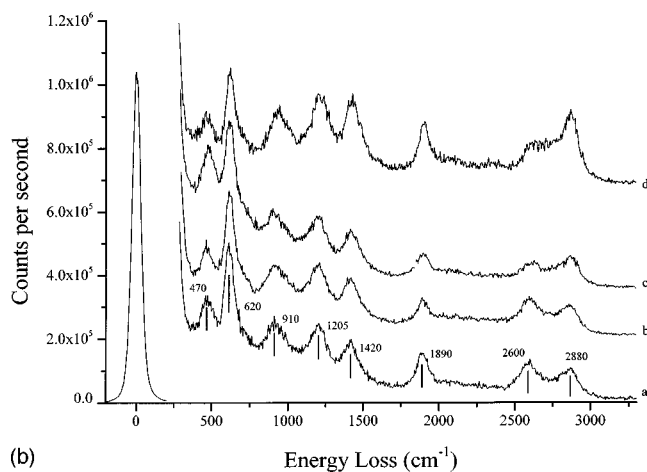
The TPD spectra of cyclobutane ($m/e=56$), collected for various initial exposures of cyclobutane at a temperature ramp rate of 5 K/s, are displayed in Fig. 1. A single desorption peak is observed at 170 K for low exposures, and is labeled as α_1 . This α_1 peak is attributed to first-order molecular desorption of monolayer cyclobutane from the Ru(001) surface. The activation energy of desorption for the α_1 desorption peak was determined, using the method of Redhead,¹⁴ to be $10\,100 \pm 150$ cal/mol. This is in good agreement with the value reported previously by Hoffmann *et al.*¹⁵ The intensity of the α_1 peak increases with increasing exposure until it saturates at an exposure of approximately 2 L. Once the α_1 peak saturates, a second desorption peak labeled as α_2 is observed. The α_2 peak, which is zeroth-order multilayer desorption of molecular cyclobutane, continues to increase at a uniform rate for all exposures investigated. The temperature of the leading edge of the α_2 desorption peak is approximately 120 K. Examination of the α_1 peak for exposures greater than 2 L reveals that the intensity of this peak decreases with increasing exposure and simultaneously downshifts in temperature. The decrease in intensity has been previously assigned to multilayer-induced decomposition of monolayer cyclobutane.¹⁶ The downshift in temperature is most likely due to repulsive adsorbate–adsorbate interactions between molecular cyclobutane and hydrocarbon moieties irreversibly bound to the surface after dissociation of a fraction of the monolayer cyclobutane. Thermal desorption spectra similar to those displayed here for $c\text{-}C_4H_8$ were also observed for $c\text{-}C_4D_8$. It should be noted that for cyclobutane exposures above 20 L, butene desorption is also observed around 200 K.¹⁷ This is the only hydrocarbon observed in the TPD experiments other than cyclobutane and its cracking fragments.

B. High-resolution electron energy loss spectroscopy

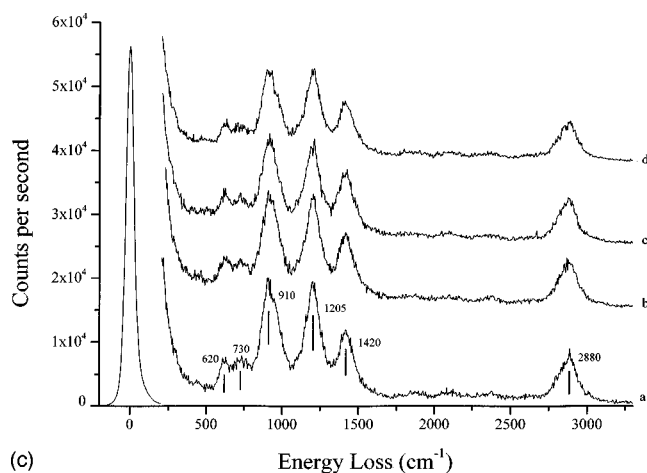
High-resolution electron energy loss spectra collected for perhydro cyclobutane adsorbed on Ru(001) at a surface



(a) HREELS spectra for a 0.7 L exposure of $c\text{-}C_4H_8$ on Ru(001) at 90 K at scattering angles of: (a) 0, (b) 5, and (c) 15°.



(b) HREELS spectra for a 1.8 L exposure of $c\text{-}C_4H_8$ on Ru(001) at 90 K at scattering angles of: (a) 0, (b) 5, (c) 10, and (d) 15°.



(c) HREELS spectra for a 3.5 L exposure of $c\text{-}C_4H_8$ on Ru(001) at 90 K at scattering angles of: (a) 0, (b) 5, (c) 10, and (d) 15°.

temperature of 90 K are displayed in Fig. 2. These HREEL spectra have been recorded at several different off-specular angles, ϕ , to elucidate better the nature of the interaction of cyclobutane with this surface. As expected, the observed loss features are similar to those reported for gas phase

TABLE I. Assignment of the observed vibrational modes for $c\text{-C}_4\text{H}_8$ ($c\text{-C}_4\text{D}_8$) on Ru(001) at 90 K for the various cyclobutane exposures indicated. (w=weak, sh=shoulder, m=multiple modes present in loss feature.)

Mode number ^a	Description	D_{2d} symmetry	Vibrational frequency (cm^{-1})					
			Gas phase IR	Gas phase Raman	0.7 L	2.0 L	3.5 L	20.0 L
...	Frustrated translation (...)	... (...)	400 (380)	470(470) ^{w,sh}
16	CH ₂ rock	B_2	626 (480)	... (...)	610 ^{w,sh} (470) ^{w,sh}	620 (470)	620 (470)	620 (470)
23	CH ₂ rock	E	749 (556)	... (...)	730(550) ^{w,sh}	730(550) ^{w,s}
22	Ring stretch	E	901 (730)	... (...)	910 (730)	910 (730)	910 (730)	890 (720)
11	Ring stretch	B_1	... (...)	926 (748)
15	Ring deformation	B_2	1001 (938)	999 (...)	980 ^{sh} (910)	980 ^{w,sh} (900) ^{sh}	980 ^{sh} (900) ^m	980 ^{sh} (900)
4	Ring stretch	A_1	... (...)	1005 (884)
7	CH ₂ twist	A_2	1225 (920)	1224 (944)	1180 ^m (910)	1205 ^m (900) ^{sh}	1205 ^m (900) ^m	1215 ^m (900)
9	CH ₂ wag	B_1	1234 (1042)	... (...)	1180 ^m (1035)	1205 ^m (1035)	1205 ^m (1035)	1215 ^m (1035)
14	CH ₂ scissor	B_2	1443 (1040)	... (...)	1405 (1095)	1420(1095) ^{sh}	1420(1095) ^m	1420 (1095)
19	CH ₂ scissor	E	1447 (1048)	1452 (1065)
...	C-H soft mode (...)	... (...)	2600(1950) ^m	2600(1950) ^m	... (...)	... (...)
18	C-H stretch	E	2887 (2129)	2883 (2127)	2880 (2140)	2880 (2140)	2880 (2140)	2880 (2140)

^aMode numbers are those used by Miller *et al.* (Ref. 19).

cyclobutane.^{18,19} The vibrational mode assignments for all spectra collected here are listed in Table I, along with the gas phase values reported in the literature. All off-specular HREEL spectra for each exposure in Fig. 2 have been normalized to have an elastically scattered peak intensity equal to that of the $\varphi=0^\circ$ spectrum in each case.

The HREEL spectra obtained for a submonolayer cyclobutane exposure of 0.7 L, at scattering angles of 0, 5, and 15° with respect to the specular angles, are shown in Fig. 2. The dominant feature in Fig. 2 is centered at 400 cm^{-1} and can be attributed to the frustrated translational mode of molecular cyclobutane, $T_z[\text{Ru}(c\text{-C}_4\text{H}_8)]$, on the surface. The frustrated translational modes of similar hydrocarbon species, such as benzene²⁰ and cyclopropane,²¹ have also been observed near this frequency. The slight shoulder on this loss feature at approximately 440 cm^{-1} can be assigned to the Ru-CO stretching mode,²² $\nu(\text{Ru-CO})$, which is present due to background adsorption of a very small amount of CO.

The low intensity shoulder at 610 cm^{-1} is assigned to the ν_{16} (mode number 16 in Table I) CH₂ rocking mode, which is observed in the gas phase at 627 cm^{-1} . At 910 cm^{-1} , a feature is observed which we can assign as the ν_{22} or ν_{11} ring stretching modes, while the feature at 980 cm^{-1} can be assigned to the ν_4 ring stretch and ν_{15} ring deformation modes. The most likely contributions to the loss feature near 1180 cm^{-1} originate from a combination of the ν_9 CH₂ wagging and ν_7 CH₂ twisting modes. The significant downshift in the modes contributing to the 1180 cm^{-1} loss from the 1225 to 1235 cm^{-1} range hints at the possibility that one of the H atoms in the CH₂ group is significantly constrained by an interaction with the substrate, an idea which will be discussed in more detail below. The loss feature with maximum intensity at 1405 cm^{-1} can be tentatively assigned to either the ν_{14} or ν_{19} scissoring modes of the CH₂ group, which is observed in the gas phase around 1450 cm^{-1} . The loss feature at 1930 cm^{-1} can be assigned to the stretching mode of contaminant CO, $\nu(\text{C-O})$, which is located at about 1960 cm^{-1} for low CO coverage on clean Ru(001).²²

The two loss features centered at 2600 and 2880 cm^{-1} can both be assigned to C-H stretching modes. The loss

centered at 2880 cm^{-1} compares well with the reported gas phase value of 2887 cm^{-1} for the ν_{18} C-H symmetric stretching mode. The loss at 2600 cm^{-1} is assigned to a softened C-H stretching mode, $\nu_{\text{soft}}(\text{C-H})$. This $\nu_{\text{soft}}(\text{C-H})$ mode, which is downshifted by 280 cm^{-1} from the observed gas phase value for ν_{18} , has been observed in other hydrocarbon-transition metal adsorption systems, including cyclopentane¹⁵ and cyclohexane^{15,23} on Ru(001) and cyclohexane on the Ni(111) and Pt(111) surfaces.²⁴ We should note that Hoffmann *et al.* did not observe a soft C-H mode for cyclobutane adsorbed on Ru(001).¹⁵ We note, however, that if the cyclobutane monolayer is prepared by overexposing the surface to cyclobutane and subsequently desorbing the multilayer to leave what is presumed to be a monolayer, a significant amount of decomposition occurs in the monolayer.¹⁶ This decomposition could change the nature of the adsorbate overlayer sufficiently that the soft mode would not be observed.

It is clear from Fig. 2(a) that the intensity of the $\nu_{\text{soft}}(\text{C-H})$ mode decreases with off-specular angle much more than does the ν_{18} mode at 2880 cm^{-1} . This behavior is strikingly similar to that observed for cyclohexane adsorbed on Ru(001),²³ and strongly suggests that the $\nu_{\text{soft}}(\text{C-H})$ mode is dominated by dipolar scattering while the ν_{18} mode is dominated by impact scattering. The strong dynamic dipole moment of the $\nu_{\text{soft}}(\text{C-H})$ mode leads us to the important conclusion that the softened C-H bond is oriented close to the surface normal and that the hydrogen atom is very close to the surface.²⁵ Kang *et al.*²⁶ calculated the H-surface distance for the soft C-H hydrogen in cyclohexane adsorbed on Pt(111) to be 2.04 \AA . They also calculated the binding energies and axial C-H bond stretching force constants for the adsorption of cyclohexane, through the interaction of the axial C-H bonds in the boat conformation, with the following Pt(111) surface sites: onefold (on-top sites), twofold (bridge sites), and threefold (hollow sites). This resulted in the onefold site being the preferred binding site of the axial C-H bond, followed by the twofold and threefold sites, respectively. Their calculation of C-H bond stretching force constants for these three different adsorption sites resulted in

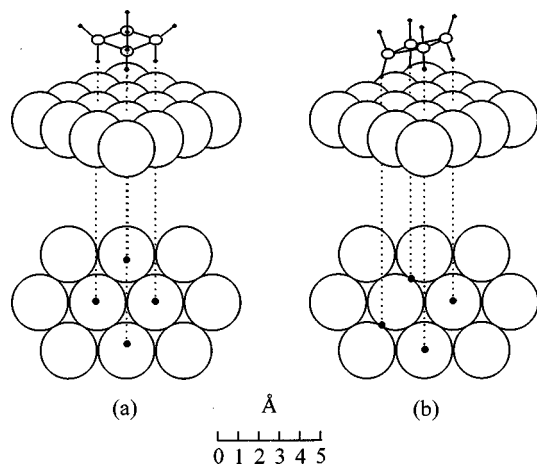


FIG. 3. Two proposed geometries for the physical adsorption of cyclobutane on the Ru(001) surface. The geometry proposed in (a) illustrates an adsorption geometry in which all four C-H bonds facing the surface interact with on-top ruthenium surface sites; (b) displays an adsorption geometry that results in the interaction of two of the C-H bonds with on-top sites and two of the C-H bonds with bridge sites.

mode softening for both the onefold and twofold sites, while the threefold site showed an increase in vibrational frequency compared to the gas phase value. Based on this, we conclude that the soft C-H modes observed here for cyclobutane are a result of C-H bonds which are most likely bound at onefold sites, but also quite possibly at twofold sites. Therefore, we propose two different adsorption geometries for cyclobutane, illustrated in Fig. 3, which are consistent with the interaction of C-H bonds with onefold and twofold ruthenium sites. The first of these, shown in Fig. 3(a), depicts an adsorption geometry in which all four C-H bonds facing the surface interact with on-top surface sites. We believe this adsorption geometry is possible due to the fact that the most stable conformation of cyclobutane in the gas phase involves puckering of the carbon skeleton by as much as 35° .²⁷ The gas phase equilibrium conformation of cyclobutane, as judged from electron diffraction and spectroscopic experiments, is nonplanar with a 35° dihedral angle. Cyclobutane molecules have C-C bond distances of 1.548 Å, C-H bond distances of 1.09 Å, and H-C-H bond angles of 110° .²⁷ Therefore, since it is plausible that the lowest energy conformation of cyclobutane adsorbed on the surface may still involve a great deal of carbon skeleton puckering, we believe that the C-H bonds on diagonal carbon atoms can bend inward, to a nearly perpendicular orientation to the surface, in order to interact with nearest-neighbor ruthenium atoms. The other two C-H bonds facing the surface can then interact with next-nearest-neighbor ruthenium atoms, cf., Fig. 3(a). These two C-H bonds, which are the front and rear C-H bonds in Fig. 3(a), are angled significantly away from the surface normal since the front and rear carbon atoms are tilted slightly away from surface due to the carbon skeleton puckering. A second proposed adsorption geometry, which involves the interaction of C-H bonds with both on-top and bridge surface sites, is displayed in Fig. 3(b). Since the bridge sites are lower in height than the on-top sites, the entire molecule is tilted in this adsorption geometry. The C-H bonds that interact with

the bridge sites are oriented almost normal to the surface. Both of these proposed adsorption geometries are consistent with the observation of the soft C-H vibrational modes and with the dipole activity of these modes. While there are certainly other possible adsorption geometries, such as adsorption with the carbon ring normal to the surface, we feel that the two proposed here are the best possibilities, based on the data collected here and on the good geometric registry of cyclobutane with these adsorption sites.

The HREEL spectra collected for a nearly saturated monolayer of cyclobutane (cyclobutane exposure of 1.8 L) for scattering angles of 0, 5, 10, and 15° with respect to the specular angle, are shown in Fig. 2(b). Many of the loss features observed at this cyclobutane coverage are identical (within 20 cm^{-1}) to those observed for submonolayer cyclobutane coverage, cf. Fig. 2(a). The sharpening of the features observed here at 1205 and 1420 cm^{-1} compared to the submonolayer coverage is significant: it implies a more narrow distribution of cyclobutane bonding sites due to locking in of bonding configurations at monolayer coverage. Centered at 470 cm^{-1} is a loss feature which most likely is a combination of the $\nu(\text{Ru}-\text{CO})$ and the $T_z[\text{Ru}-(c\text{-C}_4\text{H}_8)]$ modes, both of which may have upshifted slightly due to lateral interactions in the saturated monolayer. At 1890 cm^{-1} we observe a mode which does not seem to exhibit the same type of dipole behavior as the $\nu(\text{C}-\text{O})$ observed at 1930 cm^{-1} for submonolayer cyclobutane coverage. This mode is thought to be a downshifted $\nu(\text{C}-\text{O})$ mode that possesses some impact activity. As in the case of submonolayer cyclobutane coverage, the soft C-H mode at 2600 cm^{-1} is dipolar active while the normal C-H mode at 2880 cm^{-1} is largely impact active.

At an exposure of 3.5 L, a cyclobutane multilayer has condensed on the Ru(001) surface at 90 K. The HREEL spectra of this thin cyclobutane multilayer, collected as a function of scattering angles ($\varphi=0, 5, 10$, and 15°), are shown in Fig. 2(c). By comparing Fig. 2(c) with the HREEL spectra in Fig. 2(b), it is obvious that the $\nu(\text{Ru}-\text{CO})$ and the $T_z[\text{Ru}-(c\text{-C}_4\text{H}_8)]$ modes are no longer present in the 400 to 500 cm^{-1} range. The absence of the frustrated translation is likely a result of having a condensed multilayer adsorbed above the monolayer adsorbates. The $\nu(\text{Ru}-\text{CO})$ mode is no longer present because background adsorption of CO onto the surface during HREELS acquisition is prevented by the condensed multilayer of cyclobutane initially adsorbed on the surface. The loss feature at 620 cm^{-1} is again attributed to the $\nu_{16}\text{ CH}_2$ rocking mode, while the new feature at 730 cm^{-1} can be assigned to the $\nu_{23}\text{ CH}_2$ rocking mode. The remaining loss features in Fig. 2(c) have the same assignments as described for the identical features shown in Fig. 2(b). Also, the HREEL spectra collected for a 20 L cyclobutane exposure are nearly identical to those displayed for the 3.5 L exposure in Fig. 2(c).

We have also collected HREEL spectra for $c\text{-C}_4\text{D}_8$ at the various coverages examined in the experiments described above for $c\text{-C}_4\text{H}_8$ in order to confirm our mode assignments. Figure 4 displays the vibrational spectra obtained for $c\text{-C}_4\text{D}_8$ in the specular direction for initial cyclobutane exposures of 0.7, 1.9, 3.5, and 20.0 L. The mode assignments for the

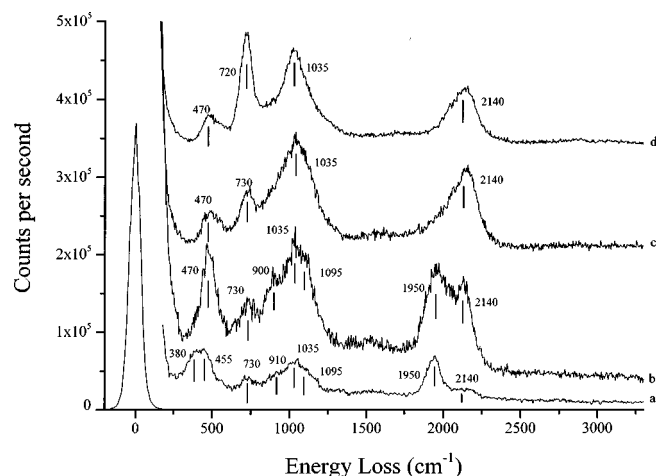


FIG. 4. HREELS spectra taken in the specular direction for the following exposures of $c\text{-C}_4\text{D}_8$ on Ru(001) at 90 K [in Langmuir (L)]: (a) 0.7, (b) 1.8, (c) 3.5, and (d) 20.0.

$c\text{-C}_4\text{D}_8$ isotopomer are also listed in Table I. For the 0.7 L exposure, displayed in Fig. 4(a), modes analogous to those observed for the perhydrido isotopomer are observed. The extremely broad loss feature between 250 and 500 cm^{-1} is believed to be a combination of three different modes: the frustrated translation $T_z[\text{Ru}(c\text{-C}_4\text{D}_8)]$ at approximately 380 cm^{-1} , the $\nu(\text{Ru-CO})$ mode at about 455 cm^{-1} , and a slight broadening at 470 cm^{-1} attributed to the ν_{16} rocking mode. Between 600 and 1200 cm^{-1} are loss features that are analogous to those in Fig. 4(b): these features are resolved more clearly in that spectrum and hence will be discussed below. The loss feature at 2140 cm^{-1} is easily assigned to the C–D stretching mode, ν_{18} . Finally, the mode at 1950 cm^{-1} is thought to be a convolution of two modes: the soft C–D stretching mode, $\nu_{\text{soft}}(\text{C-D})$, and the $\nu(\text{C-O})$ stretching mode that is located in this vicinity.

Examination of the HREEL spectrum in Fig. 4(b) corresponding to a saturated monolayer coverage enables identification of additional loss features that were not resolved in Fig. 4(a). The intense loss feature centered at 470 cm^{-1} is again thought to be the convolution of the $T_z[\text{Ru}(c\text{-C}_4\text{D}_8)]$, $\nu(\text{Ru-CO})$, and ν_{16} modes. We believe that the slight upshift in frequency of this broad peak as compared to the submonolayer coverage in Fig. 4(a) can be attributed to a slight upshift in frequency of both the $T_z[\text{Ru}(c\text{-C}_4\text{D}_8)]$ and $\nu(\text{Ru-CO})$ modes, as was believed to be the case for $c\text{-C}_4\text{H}_8$ as well. At 730 cm^{-1} we observe a ring stretching mode which agrees well with the reported gas phase values of 730 cm^{-1} for ν_{22} or 748 cm^{-1} for ν_{11} . The shoulder at 900 cm^{-1} is difficult to assign conclusively since there are many gas phase modes in this vicinity. We tentatively assign this feature to a combination of the ν_4 and ν_{15} ring modes and the ν_7 CD_2 twisting mode. The loss at 1035 cm^{-1} can be assigned to the ν_9 CD_2 wagging mode, while the shoulder at 1095 cm^{-1} is believed to be either the ν_{14} or ν_{19} CD_2 scissoring modes. The last two loss features in this spectrum, centered at 1950 and 2140 cm^{-1} , can again be attributed to the convolution of the $\nu_{\text{soft}}(\text{C-D})$ and $\nu(\text{C-O})$ modes and the ν_{18} mode, respectively.

Spectra (c) and (d) of Fig. 4, collected at exposures of 3.5 and 20.0 L, respectively, are virtually identical except for the slightly better resolution attained in spectrum (d). The broad loss feature centered at 470 cm^{-1} is assigned primarily to the ν_{16} CD_2 rocking mode, which is observed at 480 cm^{-1} in the gas phase. The shoulder on this mode extending to just above 550 cm^{-1} can also be assigned to a CD_2 rocking mode, ν_{23} , as judged by the observance of this mode at 556 cm^{-1} in the gas phase. The extremely broad loss feature extending from approximately 800 to 1200 cm^{-1} is assigned, by comparison with the spectra obtained for the perhydrido isotopomer, to a convolution of many vibrational modes. Those modes which we expect to contribute to this loss feature include the ν_4 ring stretching mode (884 cm^{-1} in the gas phase), the ν_7 CD_2 twisting mode (920 cm^{-1}), the ν_9 CD_2 wagging mode (1042 cm^{-1}), and the ν_{14} or ν_{19} CD_2 scissoring modes (1084 cm^{-1}).

The extensive HREEL spectra collected here for both cyclobutane isotopomers makes it possible for us to assign the observed modes with confidence. The collection of off-specular vibrational spectra provides insight into the bonding geometry of cyclobutane adsorbed on Ru(001) at 90 K. More specifically, the dipole activity of the soft C–H mode in the monolayer adsorption state leads us to believe that the adsorption geometry of cyclobutane involves the interaction of the C–H bonds facing the surface with on-top and bridge surface sites, as illustrated in Fig. 3. The strong shift in the vibrational frequency of the soft C–H mode from the reported gas phase value indicates that the interaction between the C–H bond and the surface is indeed a strong one. We have previously reported that the adsorption of a monolayer of cyclobutane and subsequent annealing results in desorption of molecular cyclobutane, except for a trivial amount (<1%) of decomposition at defect sites.¹⁶ From this, we can conclude that the strong interaction between the C–H bond and the surface does not result in the dissociation of cyclobutane via C–H bond cleavage. Below, we will confirm that the dissociative chemisorption of cyclobutane occurs via C–C bond cleavage.

C. Activation of cyclobutane at elevated surface temperature

The initial probability of trapping-mediated dissociative chemisorption of both $c\text{-C}_4\text{H}_8$ and $c\text{-C}_4\text{D}_8$ has been measured as a function of surface temperature between 190 and 1200 K. Arrhenius constructions for both isotopomers of cyclobutane are displayed as a function of reciprocal surface temperature in Fig. 5. The experimentally determined reaction probabilities of $\sim 4.5 \times 10^{-2}$ and $\sim 2.1 \times 10^{-2}$ for $c\text{-C}_4\text{H}_8$ and $c\text{-C}_4\text{D}_8$, respectively, are remarkably constant over the entire temperature range studied. Linear least-squares fits to each of the Arrhenius constructions displayed in Fig. 5 result in slopes of -10 ± 30 and 80 ± 40 cal/mol, and intercepts of 21 ± 2 and 47 ± 4 , for $c\text{-C}_4\text{H}_8$ and $c\text{-C}_4\text{D}_8$, respectively. The quoted uncertainties represent one standard deviation in the reported values.

The experimental conditions of this study, namely, low pressure and low incident kinetic energy of the cyclobutane, which is characterized by a Maxwell–Boltzmann distribution

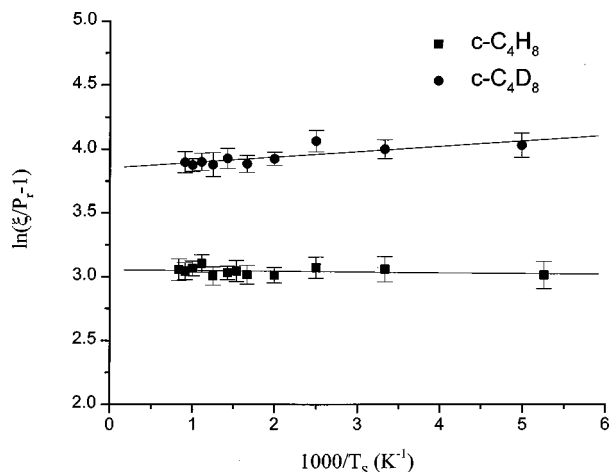
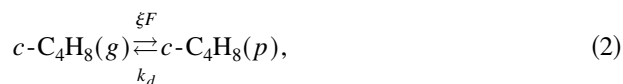


FIG. 5. Arrhenius plot, suggested by the kinetic model of Eq. (8), displaying $\ln(\xi/P_r - 1)$ vs reciprocal surface temperature for both $c\text{-C}_4\text{H}_8$ and $c\text{-C}_4\text{D}_8$ on Ru(001). The error bars represent one standard deviation in the measured probability at each temperature.

at 300 K, enable quantification of the trapping-mediated dissociative chemisorption of cyclobutane on the Ru(001) surface.²⁸ The elementary reaction steps describing cyclobutane dissociation via ring opening C–C bond cleavage may be written as¹



where molecular cyclobutane impinging from the gas phase with impingement rate F traps with probability ξ into the physically adsorbed state and then either desorbs with rate coefficient k_d or reacts with rate coefficient k_r to a dissociatively chemisorbed product which is most likely a saturated C_4 metallacycle surface intermediate.¹⁷ The chemisorbed metallacycle then undergoes dehydrogenation, depending on the surface temperature, to surface carbon and hydrogen adatoms, the latter of which desorb as H_2 at elevated surface temperature. The time rate of change of the fractional surface coverage of physically adsorbed cyclobutane can be expressed as²⁹

$$\frac{d\theta_{c\text{-C}_4\text{H}_8(p)}}{dt} = \xi F - k_r \theta_{c\text{-C}_4\text{H}_8(p)} - k_d \theta_{c\text{-C}_4\text{H}_8(p)}. \quad (4)$$

Since the fractional coverage of physically adsorbed cyclobutane under our experimental conditions is always less than 10^{-4} , we may use a pseudo-steady-state analysis to determine the coverage of physically adsorbed cyclobutane. Since the rate-limiting step in the reaction of cyclobutane with the Ru(001) surface is the initial cleavage of a C–C bond, we may write the probability of reaction of cyclobutane as

$$P_r = \frac{R_r}{F} = \frac{k_r \theta_{c\text{-C}_4\text{H}_8(p)}}{F} = \frac{\xi k_r}{k_r + k_d}, \quad (5)$$

where R_r is the rate of reaction of cyclobutane via C–C bond cleavage. The elementary rate coefficients, k_i , are of the Polanyi–Wigner form, i.e.,

$$k_i = k_i^{(0)} \exp\left[\frac{-E_i}{k_B T_s}\right], \quad (6)$$

where E_i is the activation energy and $k_i^{(0)}$ is the preexponential factor of the rate coefficient. Rearrangement of Eq. (5) and substitution of Eq. (6) for each of the rate coefficients imply that

$$\left[\frac{\xi}{P_r} - 1\right] = \frac{k_d^{(0)}}{k_r^{(0)}} \exp\left[\frac{-(E_d - E_r)}{k_B T_s}\right], \quad (7)$$

or, equivalently,

$$\ln\left[\frac{\xi}{P_r} - 1\right] = \ln\left[\frac{k_d^{(0)}}{k_r^{(0)}}\right] + \left[\frac{-(E_d - E_r)}{k_B T_s}\right], \quad (8)$$

which is the Arrhenius form used in plotting the data of Fig. 5. Since we have experimentally determined the initial probability of dissociative chemisorption, P_r , as a function of surface temperature, T_s , we now only need to know the value of ξ in order to determine the values for $E_d - E_r$ and $k_d^{(0)}/k_r^{(0)}$ for each isotopomer. We can reasonably assume a value of unity for ξ for the gas translational energies employed in this study. This assumption is based on molecular beam studies which have quantified the trapping probability of various alkanes,^{30–34} including cyclopropane,³⁵ on transition metal surfaces and on recent work involving the trapping-mediated dissociative chemisorption of cyclopropane on Ru(001).⁵ It is now clear that the slope of the Arrhenius plot in Fig. 5 is equal to $-(E_d - E_r)/(k_B)$, while the intercept is equal to $\ln(k_d^{(0)}/k_r^{(0)})$.

For $c\text{-C}_4\text{H}_8$, the measured slope of -10 cal/mol is equal to $-(E_d - E_r)$ and the measured intercept gives a ratio of $k_d^{(0)}/k_r^{(0)}$, which is equal to 21 ± 2 . Making use of the independently measured value of $E_d = 10\,100 \pm 150$ cal/mol, we find that $E_r = 10\,090 \pm 180$ cal/mol for the perhydroisoisotopomer. Similarly, for $c\text{-C}_4\text{D}_8$, we find that $k_d^{(0)}/k_r^{(0)}$ is equal to 47 ± 4 and $E_r = 10\,180 \pm 190$ cal/mol.

The lack of a significant kinetic isotope effect in the activation barriers which describe the trapping-mediated dissociative chemisorption of the two isotopomers of cyclobutane on Ru(001) implies that ring-opening C–C bond cleavage is the initial dissociation step in this reaction.⁵ If C–H bond cleavage were the active channel for initial dissociative chemisorption of cyclobutane, we would expect the difference in activation energies between $c\text{-C}_4\text{D}_8$ and $c\text{-C}_4\text{H}_8$ to be approximately 1100 cal/mol, which is the ground-state zero-point energy difference between C–H and C–D bonds.³⁶ The very small difference in the activation barriers of $c\text{-C}_4\text{D}_8$ and $c\text{-C}_4\text{H}_8$ may be attributed to a weak secondary isotope effect.³⁷ Figure 6 displays the potential energy diagram describing the dissociative chemisorption of $c\text{-C}_4\text{H}_8$, via initial C–C bond cleavage, on the Ru(001) surface. The relatively constant experimental values obtained for P_r over the temperature range of 190 to 1200 K are a result of the special case where the desorption and reaction activation barriers are nearly identical.

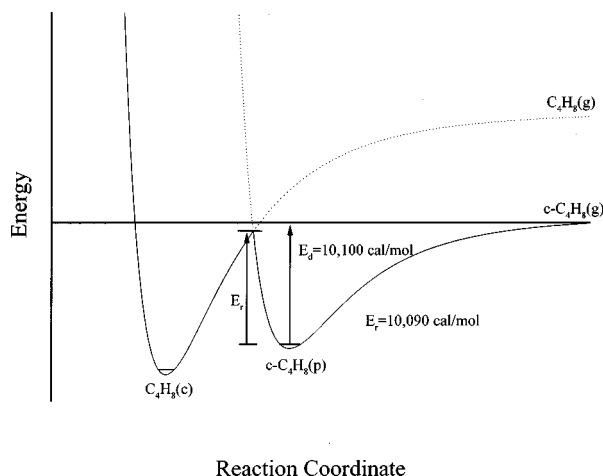


FIG. 6. Reaction coordinate diagram comparing the activation barriers for desorption and dissociative chemisorption of *c*-C₄H₈ on Ru(001). The gas phase zero reference energy is the cyclobutane molecule infinitely far from the surface.

The measured preexponential ratios of 21 and 47 for *c*-C₄H₈ and *c*-C₄D₈, respectively, are the ratios of the preexponential factors for desorption to the preexponential factors for reaction for each isotopomer. Since the activation of cyclobutane on Ru(001) is essentially temperature invariant, the ratio of the preexponential factors for desorption relative to that for reaction is approximately equal to the ratio of the rate of desorption relative to the rate of reaction. Qualitatively, these observed values are approximately those which would be expected by considering the greater entropy associated with the transition state for desorption relative to the transition state for reaction of cyclobutane via C–C bond cleavage.³⁸ The difference between the preexponential factor ratios for the cyclobutane isotopomers can be quantitatively explained using statistical mechanics combined with transition state theory.³⁹ First, we can write the following expression for the ratio of the preexponential factor for desorption, $k_d^{(0)}$, to the preexponential factor for reaction, $k_r^{(0)}$,

$$\frac{k_d^{(0)}}{k_r^{(0)}} = \frac{(q_d^\ddagger/q_{d, is})}{(q_r^\ddagger/q_{r, is})} = \frac{q_d^\ddagger}{q_r^\ddagger}, \quad (9)$$

where q_d^\ddagger is the partition function for the transition state for desorption, q_r^\ddagger is the partition function for the transition state for reaction, $q_{d, is}$ is the partition function for the initial adsorption state of cyclobutane prior to desorption and $q_{r, is}$ is the partition function for the initial adsorption state of cyclobutane prior to reaction. Because reaction and desorption occur from the same initial cyclobutane state, $q_{d, is} = q_{r, is}$, and the expression in Eq. (9) reduces to simply the ratio of the transition state partition function for desorption relative to that for reaction. The ratio of preexponential factors of the rate coefficient of desorption relative to that of reaction for *c*-C₄D₈ (subscript *D*) compared to *c*-C₄H₈ (subscript *H*) is given by

$$\frac{(k_d^{(0)}/k_r^{(0)})_D}{(k_d^{(0)}/k_r^{(0)})_H} = \frac{(q_d^\ddagger/q_r^\ddagger)_D}{(q_d^\ddagger/q_r^\ddagger)_H}. \quad (10)$$

If we reasonably assume that the transition state for reaction is localized on the surface with only vibrational degrees of freedom and the transition state for desorption is delocalized on the surface with three rotational and two translational degrees of freedom, we can write

$$(q_d^\ddagger/q_r^\ddagger)_i = \left[\frac{(q_{\text{rot}}^\ddagger)^3 (q_{\text{trans}}^\ddagger)^2}{\prod_{j=1}^5 q_{\text{vib}, j}^\ddagger} \right]_i, \quad (11)$$

where the five vibrational degrees of freedom in the denominator are frustrated translations and rotations of the molecule in the transition state for dissociative chemisorption, and *i* is either *H* or *D*. After substitution of Eq. (11) into Eq. (10) and cancellation of many identical terms in the translational and rotational partition functions,^{37,39} we obtain the following expression:

$$\frac{(k_d^{(0)}/k_r^{(0)})_D}{(k_d^{(0)}/k_r^{(0)})_H} \cong \left[\frac{m_D}{m_H} \right] \left[\frac{(I_X I_Y I_Z)_D}{(I_X I_Y I_Z)_H} \right]^{1/2} \left[\frac{(\prod_{j=1}^5 q_{\text{vib}, j}^\ddagger)_H}{(\prod_{j=1}^5 q_{\text{vib}, j}^\ddagger)_D} \right]. \quad (12)$$

The frequencies of the three frustrated rotations and two frustrated translations, $q_{\text{vib}, j}^\ddagger$, are approximately the same for both isotopomers since they involve motion of the entire molecule. Therefore, Eq. (12) reduces to

$$\frac{(k_d^{(0)}/k_r^{(0)})_D}{(k_d^{(0)}/k_r^{(0)})_H} \cong \left[\frac{m_D}{m_H} \right] \left[\frac{(I_X I_Y I_Z)_D}{(I_X I_Y I_Z)_H} \right]^{1/2}. \quad (13)$$

After substitution of the mass ($m_D = 64$, $m_H = 56$ amu) and the moments of inertia (*c*-C₄H₈: $I_X = I_Y = 47.27$ amu Å², $I_Z = 74.66$ amu Å²; *c*-C₄D₈: $I_X = I_Y = 67.03$ amu Å², $I_Z = 96.93$ amu Å²)¹⁹ of each isotopomer into Eq. (13), we obtain

$$\frac{(k_d^{(0)}/k_r^{(0)})_D}{(k_d^{(0)}/k_r^{(0)})_H} \cong 1.85. \quad (14)$$

This value compares extremely well with the experimentally measured ratio of

$$\frac{(k_d^{(0)}/k_r^{(0)})_D}{(k_d^{(0)}/k_r^{(0)})_H} = 2.2 \pm 0.4, \quad (15)$$

which leads us to believe that the measured ratio is consistent with a transition state for desorption with three rotational degrees of freedom and two translational degrees of freedom parallel to the surface.

Evidently, the preference for C–C bond cleavage over C–H bond cleavage is a result of the ring strain present in molecular cyclobutane. The strain energy of cyclobutane may be defined as the difference between the heat of combustion for cyclobutane and the heat of combustion for a hypothetical, unstrained cyclobutane.⁴ The strain energy of cyclobutane is 26.4 kcal/mol, while the strain energy of cyclopropane is 27.6 kcal/mol. Jachimowski *et al.*⁵ report an activation energy, E_r , of 9470 cal/mol for the C–C bond cleavage of cyclopropane on Ru(001), while the value determined here for cyclobutane on Ru(001) is 10 090 cal/mol. The 1.2 kcal/mol of additional ring strain in molecular cyclopropane compared to cyclobutane results in a 0.6 kcal/mol

lower activation barrier to dissociative chemisorption of cyclopropane relative to that for cyclobutane. These data indeed suggest that ring strain plays a role in the lower barrier to dissociative chemisorption.

IV. CONCLUSIONS

Following the adsorption of both *c*-C₄H₈ and *c*-C₄D₈ at 90 K on Ru(001), we have employed HREELS and TPD to determine the nature of the interaction of cyclobutane with the surface. From these results, we have determined that the adsorption of cyclobutane on this surface is molecular, except for a small amount of dissociation at surface defect sites. The loss features observed in the HREELS spectra compiled for both isotopomers are consistent with reported gas phase values except for two features: a frustrated translational mode of molecular cyclobutane and a soft C–H mode attributed to the strong interaction of C–H bonds with either on-top or bridge ruthenium surface sites. The dipole activity and intensity of the soft C–H mode, combined with the observed vibrational losses consistent with those reported for gas phase cyclobutane, suggest that cyclobutane is physically adsorbed such that the soft C–H bonds are oriented nearly normal to the surface.

At surface temperatures from 190 to 1200 K, we have measured the initial probability of dissociative chemisorption of both perhydrido and perdeutero cyclobutane isotopomers on Ru(001). The activation energies of 10 090 and 10 180 cal/mol for *c*-C₄H₈ and *c*-C₄D₈, respectively, are with respect to the bottom of the physically adsorbed well. We believe that the absence of a kinetic isotope effect here strongly implicates C–C bond cleavage as the initial dissociation step. The ratio of the preexponential factor for desorption to the preexponential factor for reaction for *c*-C₄H₈ is 21 while this ratio is 47 for the *c*-C₄D₈ isotopomer. We believe that the difference in preexponential ratios for the different cyclobutane isotopomers is consistent with a transition state for desorption with two translational degrees of freedom parallel to the surface and three rotational degrees of freedom.

ACKNOWLEDGMENTS

This research was supported by the Department of Energy under Grant No. DE-FG03-89ER14048 and by the National Science Foundation under Grant No. CHE-9626338. C.H. and M.W. also received support from the NSF predoctoral fellowship program.

- ¹D. F. Johnson and W. H. Weinberg, *J. Chem. Phys.* **103**, 5833 (1995).
- ²D. F. Johnson and W. H. Weinberg, *J. Chem. Soc., Faraday Trans.* **91**, 3695 (1995).
- ³D. Cremer and J. Gauss, *J. Am. Chem. Soc.* **108**, 7467 (1986).
- ⁴L. G. Wade, Jr., *Organic Chemistry*, 2nd ed. (Prentice-Hall, Englewood Cliffs, NJ, 1991).
- ⁵T. A. Jachimowski and W. H. Weinberg, *Surf. Sci.* **370**, 71 (1997).
- ⁶M. J. Weiss, C. J. Hagedorn, and W. H. Weinberg, *J. Vac. Sci. Technol. A* (in press).
- ⁷J. L. Taylor, D. E. Ibbotson, and W. H. Weinberg, *J. Chem. Phys.* **69**, 4298 (1978).
- ⁸J. R. Engstrom and W. H. Weinberg, *Rev. Sci. Instrum.* **55**, 404 (1984).
- ⁹T. E. Madey, H. A. Englehardt, and D. Menzel, *Surf. Sci.* **48**, 304 (1975).
- ¹⁰D. S. Connor and E. R. Wilson, *Tetrahedron Lett.* **49**, 4925 (1967).
- ¹¹T. A. Jachimowski and W. H. Weinberg, *Surf. Sci.* **372**, 145 (1997).
- ¹²H. Pfnur and D. Menzel, *Surf. Sci.* **148**, 411 (1984).
- ¹³E. D. Williams and W. H. Weinberg, *Surf. Sci.* **82**, 93 (1979).
- ¹⁴P. A. Redhead, *Vacuum* **12**, 203 (1962).
- ¹⁵F. M. Hoffmann and T. H. Upton, *J. Phys. Chem.* **88**, 6209 (1984).
- ¹⁶C. J. Hagedorn, M. J. Weiss, and W. H. Weinberg, *J. Am. Chem. Soc.* **120**, 11824 (1998).
- ¹⁷M. J. Weiss, C. J. Hagedorn, P. J. Mikesell, R. D. Little, and W. H. Weinberg, *J. Am. Chem. Soc.* **120**, 11812 (1998).
- ¹⁸R. C. Lord and I. Nakagawa, *J. Chem. Phys.* **39**, 2951 (1963).
- ¹⁹F. A. Miller, R. J. Capwell, R. C. Lord, and D. G. Rea, *Spectrochim. Acta A* **28**, 603 (1972).
- ²⁰S. Lehwald, H. Ibach, and J. E. Demuth, *Surf. Sci.* **78**, 577 (1978).
- ²¹T. E. Felter, F. M. Hoffmann, P. A. Thiel, and W. H. Weinberg, *Surf. Sci.* **130**, 163 (1983).
- ²²P. He, H. Dietrich, and K. Jacobi, *Surf. Sci.* **345**, 241 (1996).
- ²³F. M. Hoffmann, T. E. Felter, P. A. Thiel, and W. H. Weinberg, *Surf. Sci.* **130**, 173 (1983).
- ²⁴J. E. Demuth, H. Ibach, and S. Lehwald, *Phys. Rev. Lett.* **40**, 1044 (1978).
- ²⁵H. Ibach and D. L. Mills, *Electron Energy Loss Spectroscopy and Surface Vibrations* (Academic, New York, 1982).
- ²⁶D. B. Kang and A. B. Anderson, *J. Am. Chem. Soc.* **107**, 7858 (1985).
- ²⁷A. Stein, C. W. Lehmann, and P. Luger, *J. Am. Chem. Soc.* **114**, 7684 (1992).
- ²⁸T. A. Jachimowski, C. J. Hagedorn, and W. H. Weinberg, *Surf. Sci.* **393**, 126 (1997).
- ²⁹K. A. Fichthorn and W. H. Weinberg, *J. Chem. Phys.* **95**, 1090 (1991).
- ³⁰C. B. Mullins and W. H. Weinberg, *J. Chem. Phys.* **92**, 3986 (1990).
- ³¹C. B. Mullins and W. H. Weinberg, *J. Vac. Sci. Technol. A* **8**, 2458 (1990).
- ³²D. Kelly and W. H. Weinberg, *J. Chem. Phys.* **105**, 271 (1996).
- ³³D. Kelly and W. H. Weinberg, *J. Chem. Phys.* **105**, 11313 (1996).
- ³⁴C. R. Arumainayagam, M. C. McMaster, G. R. Schoofs, and R. J. Madix, *Surf. Sci.* **222**, 213 (1989).
- ³⁵D. Kelly and W. H. Weinberg, *J. Chem. Phys.* **105**, 7171 (1996).
- ³⁶R. W. Verhoef, D. Kelly, C. B. Mullins, and W. H. Weinberg, *Surf. Sci.* **311**, 196 (1994).
- ³⁷*Isotope Effects in Chemical Reactions*, edited by C. J. Collins and N. S. Bowman (Van Nostrand Reinhold, New York, 1970).
- ³⁸C. T. Campbell, Y.-K. Sun, and W. H. Weinberg, *Chem. Phys. Lett.* **179**, 53 (1991).
- ³⁹K. J. Laidler, *Chemical Kinetics*, 3rd ed. (Harper Collins, New York, 1987).